

Figure S1

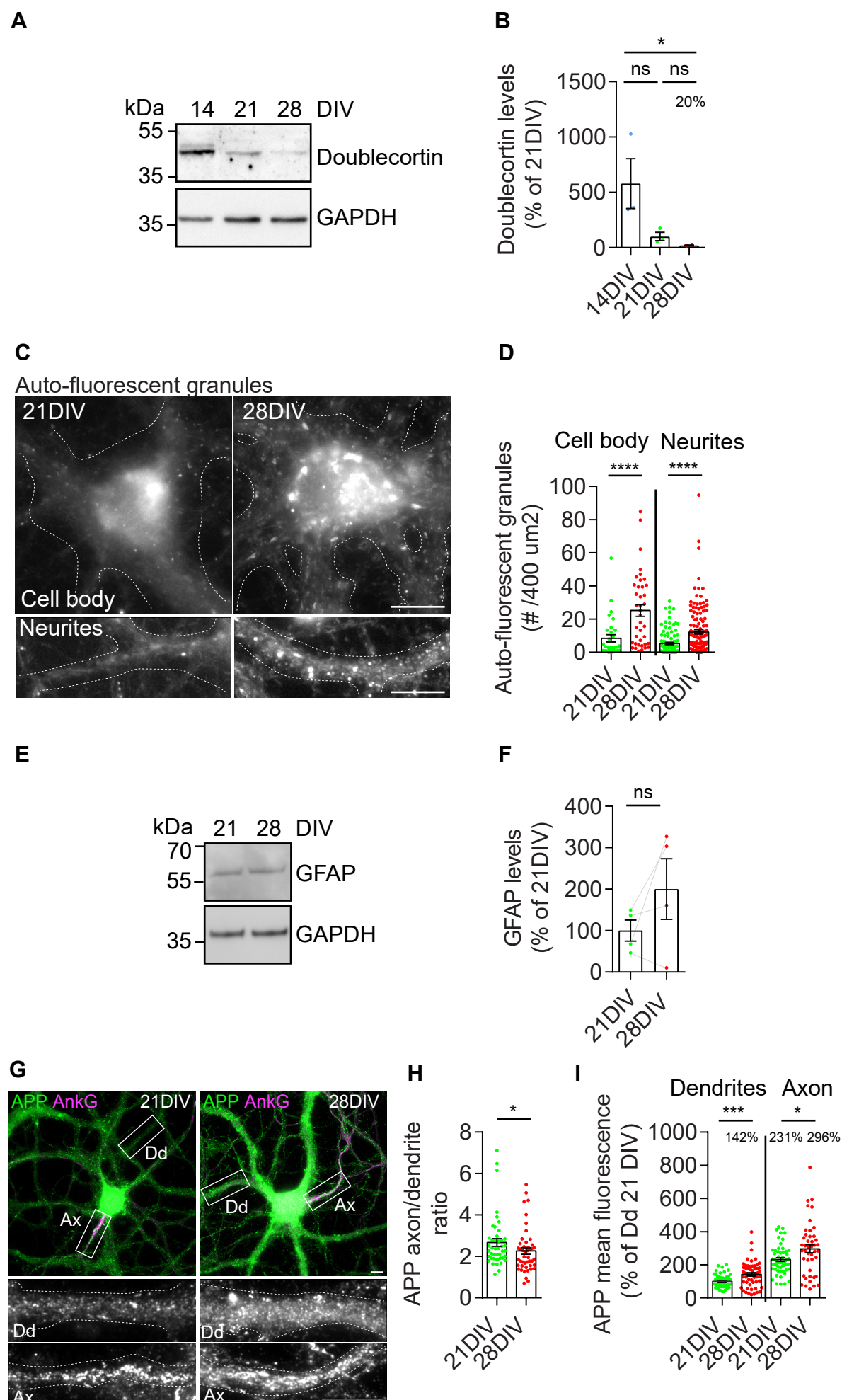
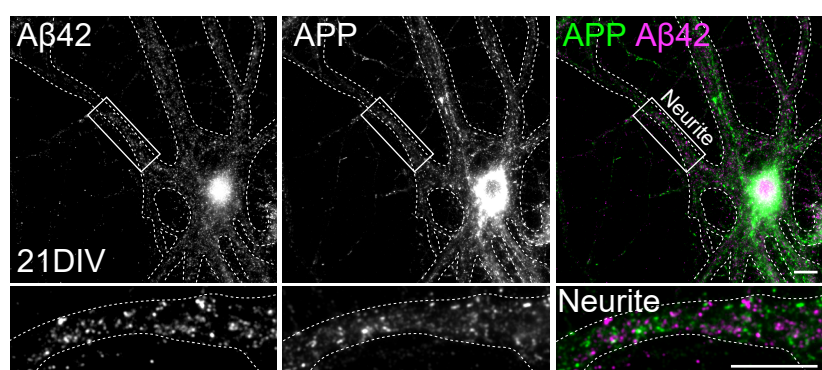


Figure S1. Aged neurons evidence canonical signs of aging and altered APP polarization.

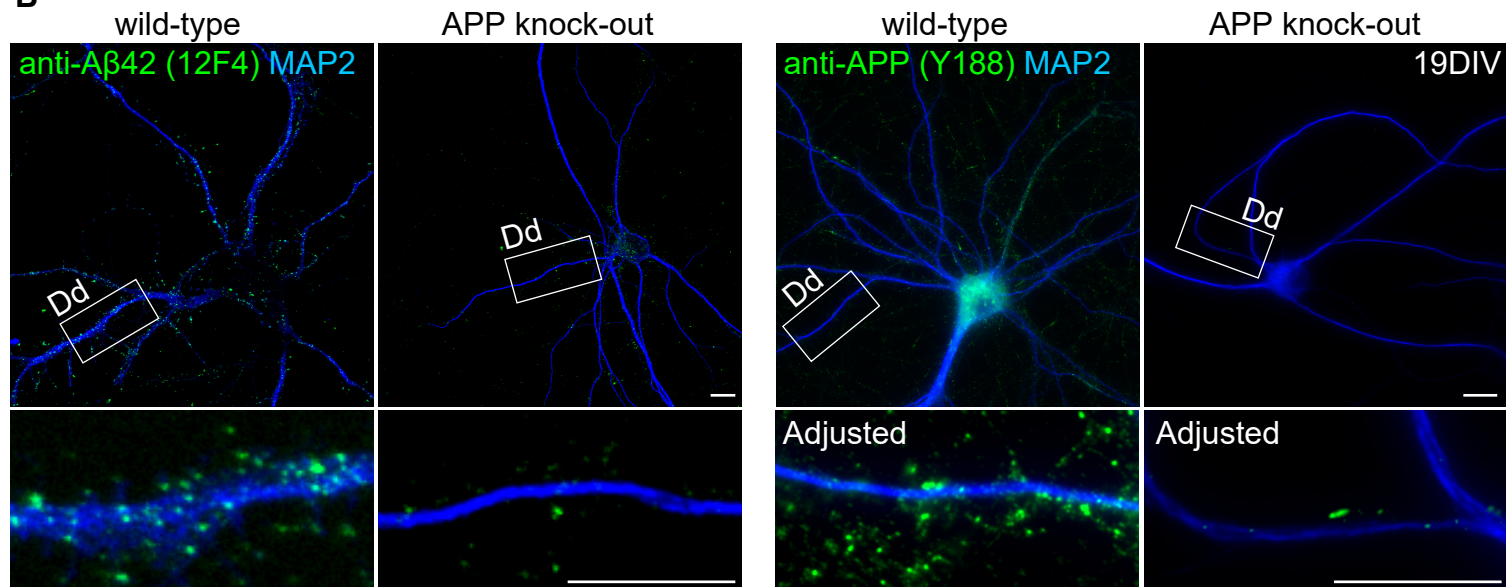
A. Endogenous doublecortin in neurons at 14 DIV, 21 DIV and 28 DIV analyzed by western blot with anti-doublecortin antibody and GAPDH as loading control. **B.** Quantification of doublecortin levels normalized to percentage of 21 DIV neurons ($n = 2-3$; ${}^{ns}P = 0.4008$ 21 DIV vs. 14 DIV; ${}^{ns}P = 0.7907$ 28 DIV vs. 21DIV; $*P = 0.0417$ 28 DIV vs. 14DIV, one-way ANOVA on ranks with *post hoc* Dunn's testing, mean \pm SEM). **C.** Auto-fluorescent aging granules, or lipofuscin, in the cell body and neurites of 21DIV and 28DIV neurons analyzed by epifluorescence microscopy. Scale bars, 10 μm . **D.** Quantification of the number of auto-fluorescent granules per area (400 μm^2) in cell body and neurites ($n=3-4$, $N_{\text{cellbody}} = 31-39$, $N_{\text{neurites}} = 60-129$, $****P_{\text{cellbody}} < 0.0001$ 28 DIV vs. 21 DIV, $****P_{\text{neurites}} < 0.0001$ 28 DIV vs. 21 DIV, Mann-Whitney test, mean \pm SEM). **E.** Endogenous glial fibrillary acidic protein (GFAP) analyzed by western blot with anti-GFAP antibody and GAPDH as loading control of neurons at 21 DIV and 28 DIV. **F.** Quantification of GFAP levels normalized to percentage of 21 DIV neurons ($n = 4$; ${}^{ns}P = 0.2271$ 28 DIV vs. 21 DIV, paired t-test, mean \pm SEM). **G.** APP (green) localization in axons and dendrites by immunofluorescence at 21 DIV and 28 DIV, with anti-APP antibody (Y188) and anti-ankyrin-G (AnkG; magenta) to identify axons, analyzed by epifluorescence microscopy. The white rectangles indicate APP (grey) localization in the magnified dendrites (Dd) and axons (Ax). Scale bar, 10 μm . **H.** Quantification of the APP axon/dendrite ratio indicating APP polarization ($n=3$, $N_{21\text{DIV}} = 44$, $N_{28\text{DIV}} = 46$; $*P = 0.0322$ 28DIV vs 21DIV, Mann-Whitney test; mean \pm SEM). **I.** Quantification of the APP mean intensity in dendrites and axons of 21DIV and 28 DIV neurons. Results were normalized to percentage of 21 DIV dendrites ($n = 4-5$, $N_{\text{dendrites}} = 57-76$; $N_{\text{axon}} = 44-55$; $***P_{\text{dendrites}} = 0.0002$ 28 DIV vs. 21 DIV dendrites, $*P_{\text{axon}} = 0.0258$ 28 DIV vs. 21 DIV axons, Mann-Whitney test, mean \pm SEM).

Figure S2

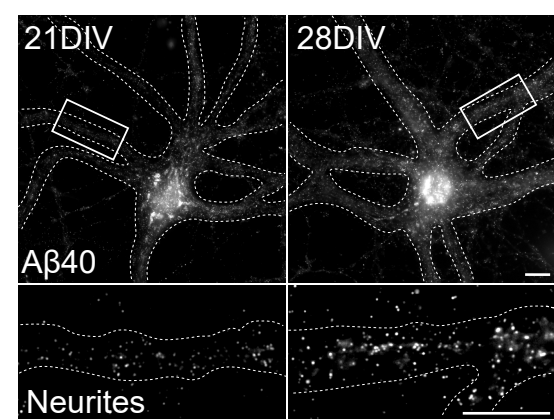
A



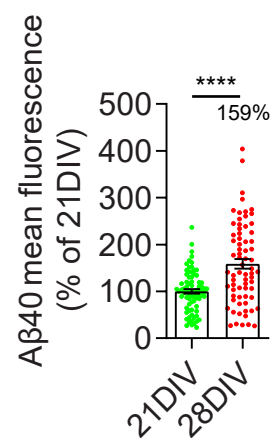
B



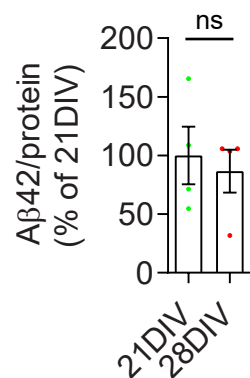
C



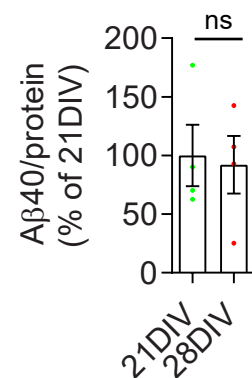
D



E



F



G

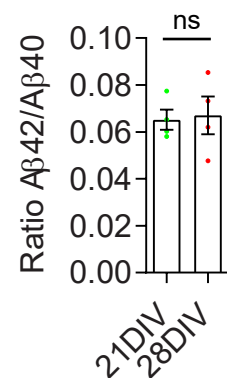


Figure S2. A β and APP antibody specificity in APP knock-out neurons, A β 40 intracellular levels and secreted A β levels.

A. A β 42 and APP co-staining with anti-A β 42 antibody (12F4) and anti-APP antibody (Y188) in 21 DIV neurons as a control for specific intracellular A β 42 detection. A β 42 (grey, first panel), APP (grey, second panel), and merged (APP green; A β 42 magenta). The white rectangles indicate the magnified regions shown below. Scale bar, 10 μ m. **B.** A β 42 and APP staining with anti-A β 42 antibody (12F4) and anti-APP antibody (Y188) in 19 DIV wild-type and APP knock-out neurons as a control for specific intracellular A β 42 (green, left panel) and APP (green, right panel) detection. MAP2 was used to label neuronal dendrites (blue). The white rectangles indicate the magnified regions shown below. Scale bar, 10 μ m. **C.** Intracellular endogenous A β 40 (grey) in neurons at 21 DIV and 28 DIV, immunolabelled with anti-A β 40 antibody, analyzed by epifluorescence microscopy. The white rectangles indicate the magnified neurites. Scale bars, 10 μ m. **D.** Quantification of A β 40 mean intensity in neurites of 21DIV and 28DIV neurons, in percentage of 21 DIV ($n = 3$, $N_{\text{neurites}} = 70-78$, $****P_{\text{neurites}} < 0.0001$ 28 DIV vs. 21 DIV neurons, unpaired t-test, mean \pm SEM). **E.** Extracellular endogenous A β 42 levels in conditioned media of neurons at 21 DIV and 28 DIV, measured by ELISA and normalized by total protein levels in the media ($n = 4$, ${}^{\text{ns}}P = 0.5459$ 28 DIV vs. 21 DIV media, paired t-test, mean \pm SEM). **F.** Extracellular endogenous A β 40 levels in the conditioned media of neurons at 21 DIV and 28 DIV, measured by ELISA and normalized by total protein levels in the media ($n = 4$, ${}^{\text{ns}}P = 0.6573$ 28 DIV vs. 21 DIV media, paired t-test, mean \pm SEM). **G.** A β 42/A β 40 ratio in the conditioned media of neurons at 21 DIV and 28 DIV, measured by ELISA and normalized by total protein levels in the media ($n = 4$, ${}^{\text{ns}}P = 0.8656$ 28 DIV vs. 21 DIV media, paired t-test, mean \pm SEM).

Figure S3

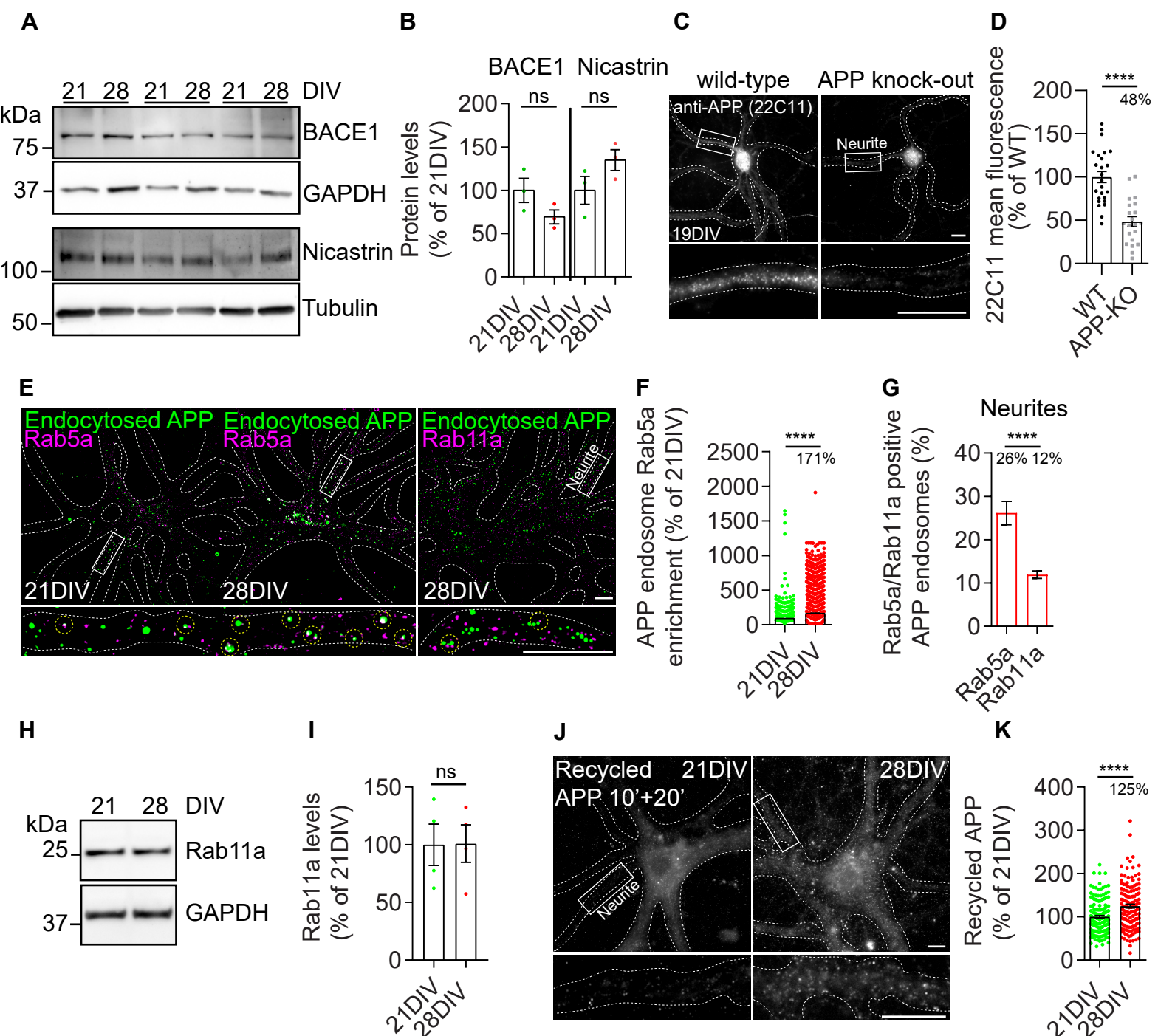


Figure S3. BACE1 and nicastrin levels, APP colocalization with Rab5a/Rab11a and APP recycling.

A. Endogenous BACE1 analyzed by western blot with anti-BACE1 antibody and GAPDH as loading control of neurons at 21 DIV and 28 DIV (top panels). Endogenous subunit of the gamma-secretase complex, nicastrin, analyzed by western blot with anti-nicastrin antibody and tubulin as loading control of neurons at 21 DIV and 28 DIV (bottom panels). **B.** Quantification of BACE1 and nicastrin levels normalized to percentage of 21 DIV neurons ($n = 3$; ${}^{ns}P_{BACE1 \text{ and } \text{nicastrin}} = 0.2000$ 28 DIV vs. 21 DIV, Mann-Whitney test, mean \pm SEM). **C.** APP staining with anti-APP antibody (22C11) in 19 DIV wild-type and APP knock-out neurons as a control for specific intracellular APP detection. The white rectangles indicate the magnified regions shown below. Scale bar, 10 μm . **D.** Quantification of 22C11 mean fluorescence intensity in 19DIV neurites of wild-type and APP knock-out (APP-KO) neurons, relative to wild-type ($n = 3$, $N_{\text{neurites}} = 21-25$, $****P_{\text{neurites}} < 0.0001$ APP-KO vs. wild-type, unpaired t-test, mean \pm SEM). **E.** APP⁺ endosomes (10'; green) and Rab5a (magenta) in neurons assessed by immunofluorescence at 21DIV and 28 DIV, with anti-Rab5a antibody. APP⁺ endosomes (10'; green) and Rab11a (magenta) in neurons assessed by immunofluorescence at 28DIV, with anti-Rab11a antibody. Both were analyzed by epifluorescence microscopy and displayed upon background subtraction. The white rectangle indicates the magnified neurite shown below. Rab5a and rab11a localization to APP⁺ endosomes (dashed yellow rings) on the magnified neurite were generated automatically by the ICY “Colocalizer” protocol. Scale bar, 10 μm . **F.** Quantification of the endosomal Rab5a, i.e. mean intensity of Rab5a per APP⁺ endosome, in percentage of 21 DIV, in neurites of 21 DIV and 28 DIV neurons ($n=3$, $N_{\text{APP}^+ \text{ endosomes}} = 11447-15437$, $****P < 0.0001$ 28 DIV vs. 21 DIV neurons, Mann-Whitney test, mean \pm SEM). **G.** Quantification of the number (mean) of Rab5a/Rab11a puncta localized to APP⁺ endosomes in percentage of APP⁺ endosomes per 28DIV neurite ($n=3$, $N_{\text{Rab5a neurites}} = 48$; $N_{\text{Rab11a neurites}} = 99$, $****P < 0.0001$ Rab11a vs. Rab5a 28DIV neurons, Mann-Whitney test, mean \pm SEM). **H.** Endogenous Rab11a analyzed by western blot with anti-Rab11a antibody and GAPDH as loading control of neurons at 21 DIV and 28 DIV. **I.** Quantification of Rab11a levels normalized to percentage of 21 DIV neurons ($n = 4$; ${}^{ns}P = 0.9476$ 28 DIV vs. 21 DIV, paired t-test, mean \pm SEM). **J.** Recycled APP (10' pulse + 20'chase) in neurites of 21 DIV and 28 DIV neurons, analyzed by epifluorescence microscopy. The white rectangle indicates the magnified neurite shown below. Scale bar, 10 μm . **K.** Quantification of the mean intensity of recycled APP in neurites of 21 DIV and 28 DIV neurons. Results were normalized to percentage of 21 DIV ($n = 3$, $N_{\text{neurites}}=143-169$; $****P_{\text{neurites}} < 0.0001$ 28 DIV vs. 21 DIV, Mann-Whitney test, mean \pm SEM).

Figure S4

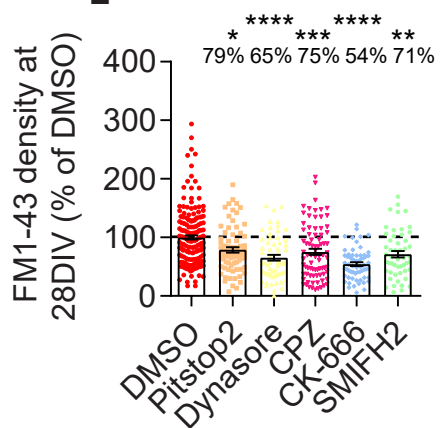
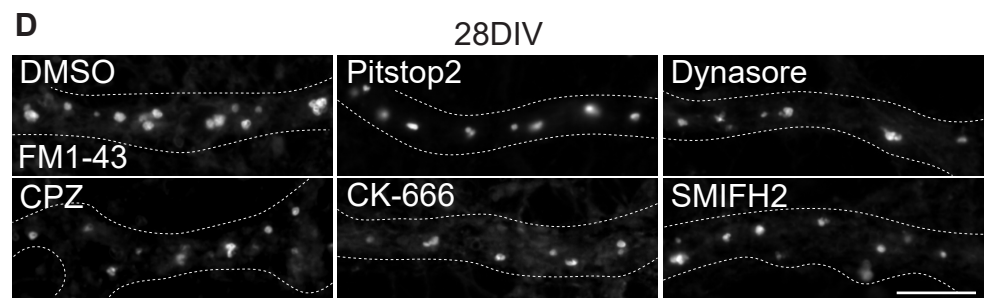
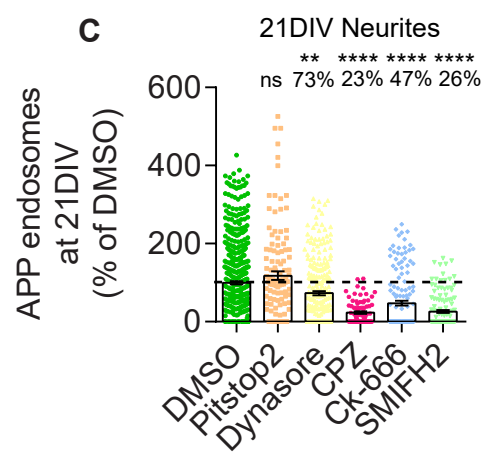
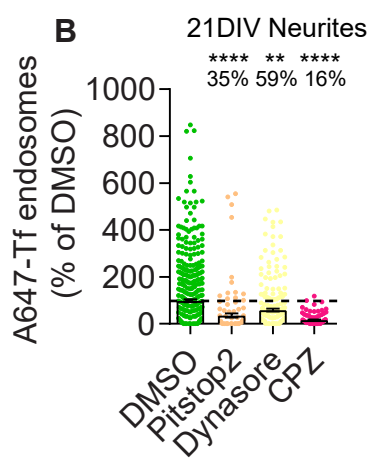
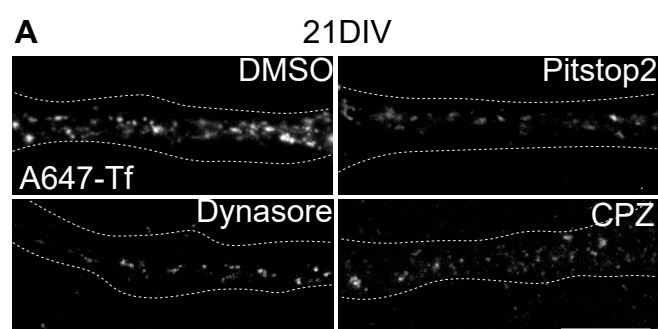


Figure S4. Transferrin, APP, and bulk endocytosis are clathrin- and dynamin-sensitive. APP endocytosis in mature neurons and bulk endocytosis in aged neurons are also dependent on actin.

A. Transferrin endocytosis in neurons pulsed with Alexa647-Tf for 10' at 21 DIV after treatment with DMSO (0.1 %), Pitstop2 (30 μ M), Dynasore (100 μ M) or CPZ (0.14 μ M). Neurons were analyzed by epifluorescence microscopy. Scale bars, 10 μ m. **B.** Quantification of the number of transferrin endosomes per area (400 μ m²) in 21 DIV neurites upon drug treatments, in percentage of DMSO (n=6, N_{DMSO}= 542, N_{Pitstop2}= 121, N_{Dynasore}= 258, N_{CPZ}= 103, , ****P< 0.0001 Pitstop2-, CPZ-treated vs. DMSO, **P = 0.0055 Dynasore-treated vs. DMSO, one-way ANOVA on ranks with *post hoc* Dunn's testing, mean \pm SEM). **C.** Quantification of the number of APP⁺ endosomes (10') per area (400 μ m²) in 21 DIV neurites upon treatment with Pitstop2 (30 μ M), Dynasore (100 μ M), CPZ (0.14 μ M), Ck-666 (50 μ M), SMIFH2 (30 μ M) and DMSO (0.1%), in percentage of control (DMSO) (n=9, N_{DMSO}= 634, N_{Pitstop2}= 118, N_{Dynasore}= 254, N_{CPZ}= 81, N_{Ck-666}= 149, N_{SMIFH2}= 136 , ^{ns}P > 0.9999 Pitstop2 vs. DMSO, ****P< 0.0001 CPZ, Ck-666-, SMIFH2 vs. DMSO, **P_{Dynasore} = 0.0015 Dynasore vs. DMSO, one-way ANOVA on ranks with *post hoc* Dunn's testing, mean \pm SEM). **D.** Bulk endocytosis in neurons pulsed with FM1-43 for 10' at 28 DIV neurites after treatment with Pitstop2 (30 μ M), Dynasore (100 μ M), CPZ (0.14 μ M), Ck-666 (50 μ M), SMIFH2 (30 μ M) and DMSO (0.1%). Neurons were analyzed by epifluorescence microscopy. Scale bars, 10 μ m. **E.** Quantification of the number of FM1-43 puncta per area (400 μ m²) in 28DIV neurites upon treatment with Pitstop2 (30 μ M), Dynasore (100 μ M), CPZ (0.14 μ M), Ck-666 (50 μ M), SMIFH2 (30 μ M) and DMSO (0.1%), in percentage of control (DMSO) (n=2, N_{DMSO}= 177, N_{Pitstop2}= 73, N_{Dynasore}= 62, N_{CPZ}= 80, N_{Ck-666}= 62, N_{SMIFH2}= 51, *P = 0.0329 Pitstop2 vs. DMSO, **P= 0.0019 SMIFH2 vs. DMSO, ***P= 0.0005 CPZ vs. DMSO, ****P< 0.0001 Dynasore and CK-666 vs. DMSOs, one-way ANOVA on ranks with *post hoc* Dunn's testing, mean \pm SEM)

Figure S5

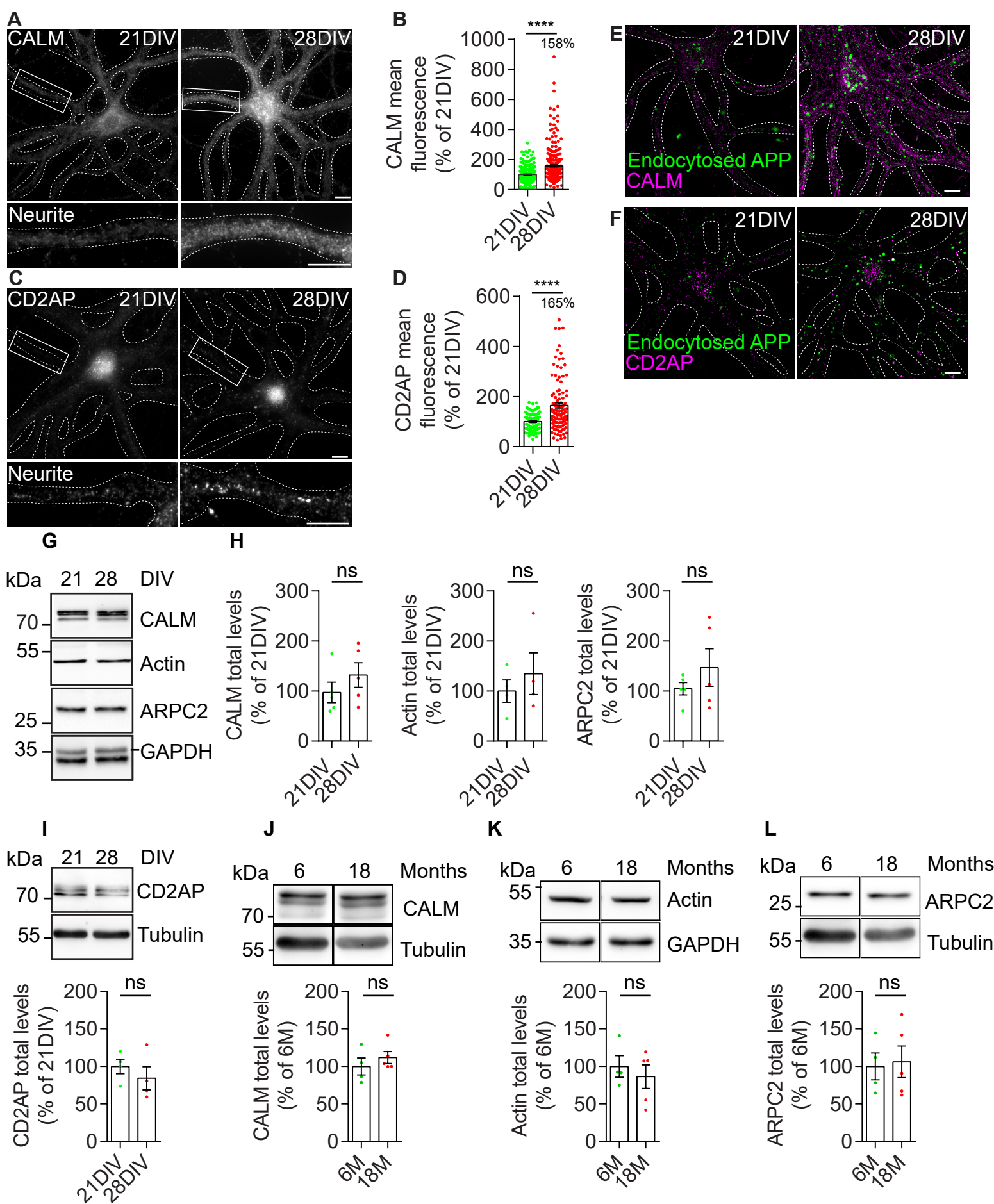


Figure S5. CALM and CD2AP increase with neuronal aging.

A. CALM distribution detected by immunofluorescence of neurons at 21 DIV and 28 DIV, analyzed by epifluorescence microscopy. The white rectangles indicate the magnified 21 DIV and 28 DIV neurites shown below. Scale bars, 10 μ m. **B.** Quantification of CALM mean intensity, normalized to percentage of 21 DIV, in 21 DIV and 28 DIV neurites ($n=5$, $N_{\text{neurites}} = 279-302$, $****P < 0.0001$ 28 DIV vs. 21 DIV, unpaired t-test, mean \pm SEM). **C.** CD2AP distribution detected by immunofluorescence of neurons at 21 DIV and 28 DIV, analyzed by epifluorescence microscopy. The white rectangles indicate the magnified 21 DIV and 28 DIV neurites shown below. Scale bars, 10 μ m. **D.** Quantification of CD2AP mean intensity, normalized to percentage of 21 DIV, in 21 DIV and 28 DIV neurites ($n=3$, $N_{\text{neurites}} = 111-122$, $****P < 0.0001$ 28 DIV vs. 21 DIV, unpaired t-test, mean \pm SEM). **E.** Enrichment of CALM on APP⁺ endosomes (22C11) in the cell body and neurites of 21 DIV and 28 DIV neurons was detected by immunofluorescence, with anti-endocytosed APP antibody (22C11; green) and anti-PICALM antibody (CALM; magenta), analyzed by epifluorescence microscopy and the images are displayed after background subtraction. Scale bar, 10 μ m. **F.** Enrichment of CD2AP on APP⁺ endosomes (22C11) in the cell body and neurites of 21 DIV and 28 DIV neurons was detected by immunofluorescence, with anti-endocytosed APP antibody (22C11; green) and anti-CD2AP antibody (magenta), analyzed by epifluorescence microscopy and the images are displayed after background subtraction. Scale bar, 10 μ m. **G.** Endogenous CALM, Actin, and ARPC2 were analyzed by western blot with anti-PICALM, anti-Actin and anti-ArpC2 antibody, and GAPDH as loading control of neurons at 21 DIV and 28 DIV. **H.** Quantification of CALM, Actin and ARPC2 levels normalized to percentage of 21 DIV neurons ($n = 4-5$; ${}^{\text{ns}}P_{\text{CALM}} = 0.2222$; ${}^{\text{ns}}P_{\text{Actin}} = 0.6571$; ${}^{\text{ns}}P_{\text{ArpC2}} = 0.6667$, 28 DIV vs. 21 DIV, Mann-Whitney test, mean \pm SEM). **I.** Endogenous CD2AP analyzed by western blot with the anti-CD2AP antibody and tubulin as loading control of neurons at 21 DIV and 28 DIV. Quantification of CD2AP levels normalized to percentage of 21 DIV neurons ($n = 4$; ${}^{\text{ns}}P = 0.4857$, 28 DIV vs. 21 DIV, Mann-Whitney test, mean \pm SEM). **J.** Endogenous CALM analyzed by western blot with anti-PICALM antibody, and tubulin as loading control of adult brains (6 M) and aged brains (18 M). Quantification of CALM levels normalized to the percentage of 6 M brain ($n = 4-5$; ${}^{\text{ns}}P = 0.5238$, 18 M vs. 6 M, Mann-Whitney test, mean \pm SEM). **K.** Endogenous Actin analyzed by western blot with anti-actin antibody, and GAPDH as loading control of adult brains (6 M) and aged brains (18 M). Quantification of actin levels normalized to the percentage of 6 M brain ($n = 4-5$; ${}^{\text{ns}}P = 0.8730$, 18 M vs. 6 M, Mann-Whitney test, mean \pm SEM). **L.** Endogenous ARPC2 analyzed by western blot with anti-ARPC2 antibody, and tubulin as loading control of adult brains (6 M) and aged brains (18 M). Quantification of ARPC2 levels normalized to the percentage of 6 M brain ($n = 4-5$; ${}^{\text{ns}}P > 0.9999$, 18 M vs. 6 M, Mann-Whitney test, mean \pm SEM).

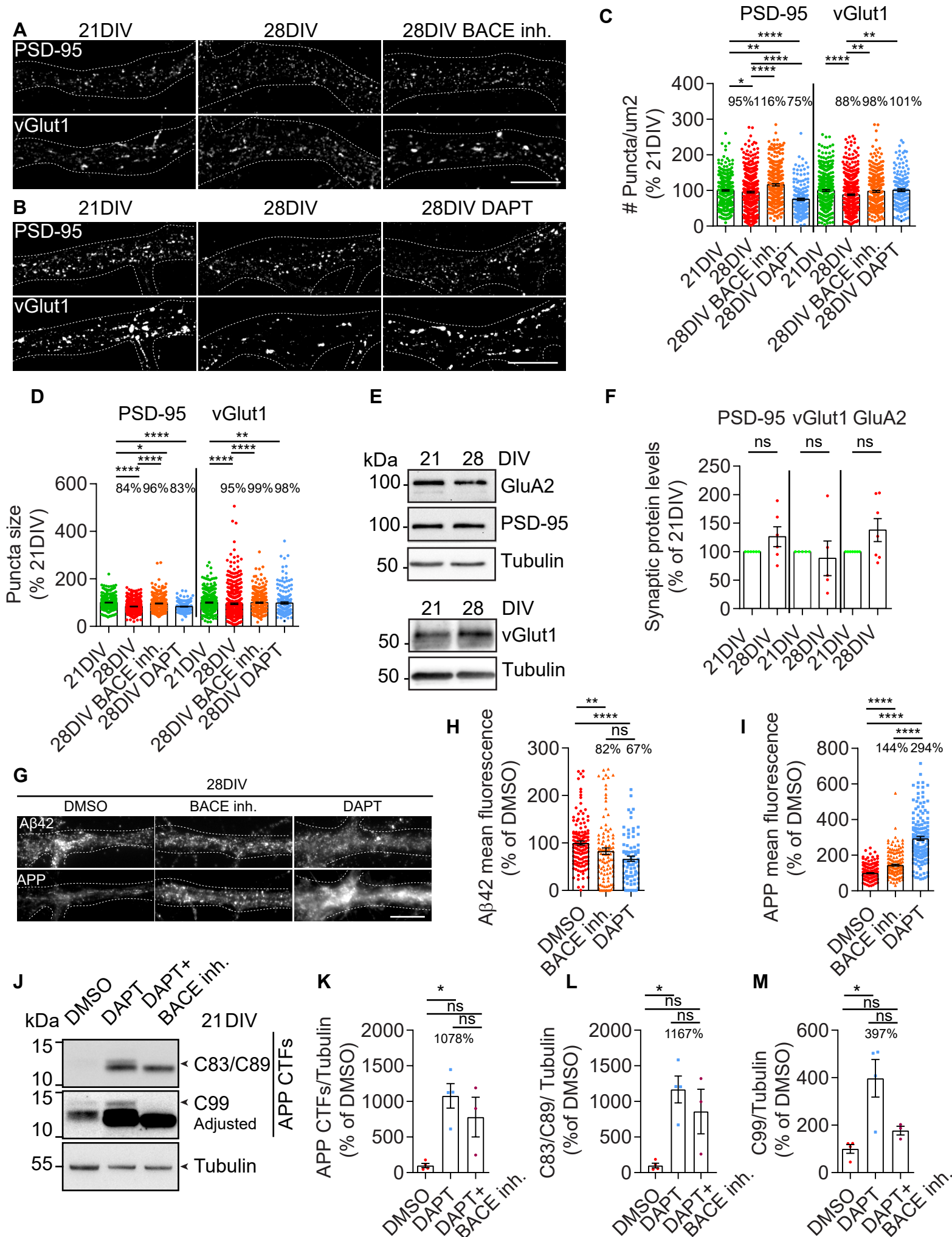
Figure S6

Figure S6. Aged synaptic proteins' puncta density and size are dependent on A β production. DAPT and BACE inhibitor are effective reducing A β levels and increasing APP processing.

A. PSD-95 and vGlut puncta in neurites of 21 DIV neurons, 28 DIV neurons, and 28 DIV neurons treated with BACE inhibitor IV, analyzed by epifluorescence microscopy, and displayed after background subtraction. Scale bar, 10 μ m. **B.** PSD-95 and vGlut puncta in neurites of 21 DIV neurons, 28 DIV neurons, and 28 DIV neurons treated with DAPT, analyzed by epifluorescence microscopy, and displayed after background subtraction. Scale bar, 10 μ m. **C.** Quantification of the number of PSD-95 and vGlut1 per 50 μ m² of neurites in 21 DIV neurites, 28 DIV neurites and DAPT or BACE inhibitor-treated 28DIV neurites. Results were normalized to percentage of 21 DIV (n=7; N_{21DIV PSD-95}=419 neurites; N_{28DIV PSD-95}=517 neurites; N_{28DIV BACE inh. PSD-95}=306 neurites; N_{28DIV DAPT PSD-95}=170 neurites; N_{21DIV vGlut}=418 neurites; N_{28DIV vGlut}=512 neurites; N_{28DIV BACE inh. vGlut}=304 neurites; N_{28DIV DAPT vGlut}=170 neurites; *P=0.0279 PSD-95 puncta density in 28 DIV vs. 21 DIV neurites, ****P < 0.0001 PSD-95 puncta density in BACE inh.-treated vs. not treated 28 DIV neurites; **P=0.0015 PSD-95 puncta density in 28 DIV BACE inh.-treated vs. not treated 21 DIV neurites; ****P < 0.0001 PSD-95 puncta density in 28 DIV DAPT-treated vs. not treated 28 DIV neurites; ****P < 0.0001 PSD-95 puncta density in 28 DIV DAPT-treated vs. not treated 21 DIV neurites; ****P < 0.0001 vGlut1 puncta density in 28 DIV vs. 21 DIV neurites, **P=0.0033 vGlut1 puncta density in BACE inh.-treated vs. not treated 28 DIV neurites; nsP=0.3202 vGlut1 puncta density in 28 DIV BACE inhibitor-treated vs. not treated 21 DIV neurites; nsP = 0.9934 vGlut1 puncta density in 28 DIV DAPT-treated vs. not treated 21 DIV neurites, **P = 0.0024 vGlut1 puncta density in DAPT-treated vs. not treated 28 DIV neurites Mann Whitney test, mean \pm SEM). **D.** Quantification of the size of PSD-95 and vGlut1 puncta in 21DIV neurites, 28 DIV neurites and DAPT or BACE inh.-treated 28DIV neurites. Results were normalized to percentage of 21 DIV (n=7; N_{21DIV PSD-95}=419 neurites; N_{28DIV PSD-95}=517 neurites; N_{28DIV BACE inh. PSD-95}=306 neurites; N_{28DIV DAPT PSD-95}=170 neurites; N_{21DIV vGlut}=418 neurites; N_{28DIV vGlut}=512 neurites; N_{28DIV BACE inh. vGlut}=304 neurites; N_{28DIV DAPT vGlut}=170 neurites; ****P < 0.0001 PSD-95 size in 28 DIV vs. 21 DIV neurites, nsP = 0.0739 PSD-95 size in DAPT-treated vs. not treated 28 DIV neurites; *P=0.0102 PSD-95 size in 28 DIV BACE inh.-treated vs. not treated 21 DIV neurites; ****P < 0.0001 PSD-95 size in BACE inh.-treated vs. not treated 28 DIV neurites; ****P < 0.0001 PSD-95 size in 28 DIV DAPT-treated vs. not treated 21 DIV neurites; ****P < 0.0001 vGlut1 size in 28 DIV vs. 21 DIV neurites, ****P < 0.0001 vGlut1 size in BACE inh.-treated vs. not treated 28 DIV neurites; nsP = 0.3114 vGlut1 size in 28 DIV BACE inh.-treated vs. not treated 21 DIV neurites; nsP = 0.3544 vGlut1 size in DAPT-treated vs. not treated 28 DIV neurites, **P = 0.0014 vGlut1 size in 28DIV DAPT-treated vs. not treated 21 DIV neurites, Mann Whitney test, mean \pm SEM). **E.** GluA2, PSD-95, and vGlut1 total levels in neurons at 21 DIV and 28 DIV, analyzed by western blot with anti-PSD-95, anti-GluA2 and anti-vGlut1 antibody. Tubulin was immunoblotted as the loading control. **F.**

Quantification of PSD-95, vGlut1 and GluA2 levels normalized to tubulin and to the percentage of 21 DIV ($n_{PSD-95} = 6$; $n_{vGlut1} = 5$; $n_{GluA2} = 7$; $^{ns}P_{PSD-95} = 0.2188$, $^{ns}P_{vGlut1} = 0.8125$, $^{ns}P_{GluA2} = 0.2188$, Wilcoxon test, mean \pm SEM). **G.** Endogenous A β 42 and APP mean intensity in neurites of 28 DIV neurons treated with DMSO (0.1%), DAPT or BACE inhibitor IV, immunolabelled with anti-A β 42 (12F4) and anti-APP (Y188) antibody, analyzed by epifluorescence microscopy. Scale bar, 10 μ m. **H.** Quantification of A β 42 mean fluorescence intensity in 28DIV neurites, in percentage of control (DMSO) ($n = 3-4$, $N_{DMSO} = 134$, $N_{DArT} = 78$, $N_{BACE\ inh.} = 99$, $****P < 0.0001$ DAPT-treated vs. DMSO, $**P = 0.0025$ BACE inh.-treated vs. DMSO, $^{ns}P = 0.4943$ DAPT-treated vs. BACE inh.-treated, one-way ANOVA on ranks with *post hoc* Dunn's testing, mean \pm SEM). **I.** Quantification of APP mean intensity in 28DIV neurites, in percentage of control (DMSO) ($n = 4-5$, $N_{DMSO} = 217$, $N_{DArT} = 151$, $N_{BACE\ inh.} = 171$, $****P < 0.0001$ DAPT-treated vs. DMSO, $****P < 0.0001$ BACE inh.-treated vs. DMSO, $****P < 0.0001$ DAPT-treated vs. BACE inh.-treated, one-way ANOVA on ranks with *post hoc* Dunn's testing, mean \pm SEM). **J.** Endogenous APP-CTFs (C191, C83/89, C99) total levels in neurons at 21 DIV treated with DMSO, DAPT, and DAPT plus BACE inhibitor IV, analyzed by western blot. Tubulin was immunoblotted as the loading control. **K.** Quantification of APP-CTFs total levels in 21DIV neurons, normalized to tubulin ($n = 3-4$; $*P_{APP\ CTFs} = 0.0315$ DAPT-treated vs. DMSO, $^{ns}P_{APP\ CTFs} = 0.1692$ DAPT plus BACE inh.-treated vs. DMSO, $^{ns}P_{APP\ CTFs} > 0.9999$ DAPT plus BACE inh.-treated vs. DAPT-treated, one-way ANOVA on ranks with *post hoc* Dunn's testing, mean \pm SEM). **L.** Quantification of C83/C89 total levels in 21DIV neurons, normalized to tubulin ($n = 3-4$; $*P_{C83/C89} = 0.0315$ DAPT-treated vs. DMSO, $^{ns}P_{C83/C89} = 0.1692$ DAPT plus BACE inh.-treated vs. DMSO, $^{ns}P_{C83/C89} > 0.9999$ DAPT plus BACE inh.-treated vs. DAPT-treated, one-way ANOVA on ranks with *post hoc* Dunn's testing, mean \pm SEM). **M.** Quantification of C99 total levels in 21DIV neurons, normalized to tubulin ($n = 3-4$; $*P_{C99} = 0.0167$ DAPT-treated vs. DMSO, $^{ns}P_{C99} = 0.3000$ DAPT plus BACE inh.-treated vs. DMSO, $^{ns}P_{C99} > 0.9999$ DAPT plus BACE inh.-treated vs. DAPT-treated, one-way ANOVA on ranks with *post hoc* Dunn's testing, mean \pm SEM).

Figure S7

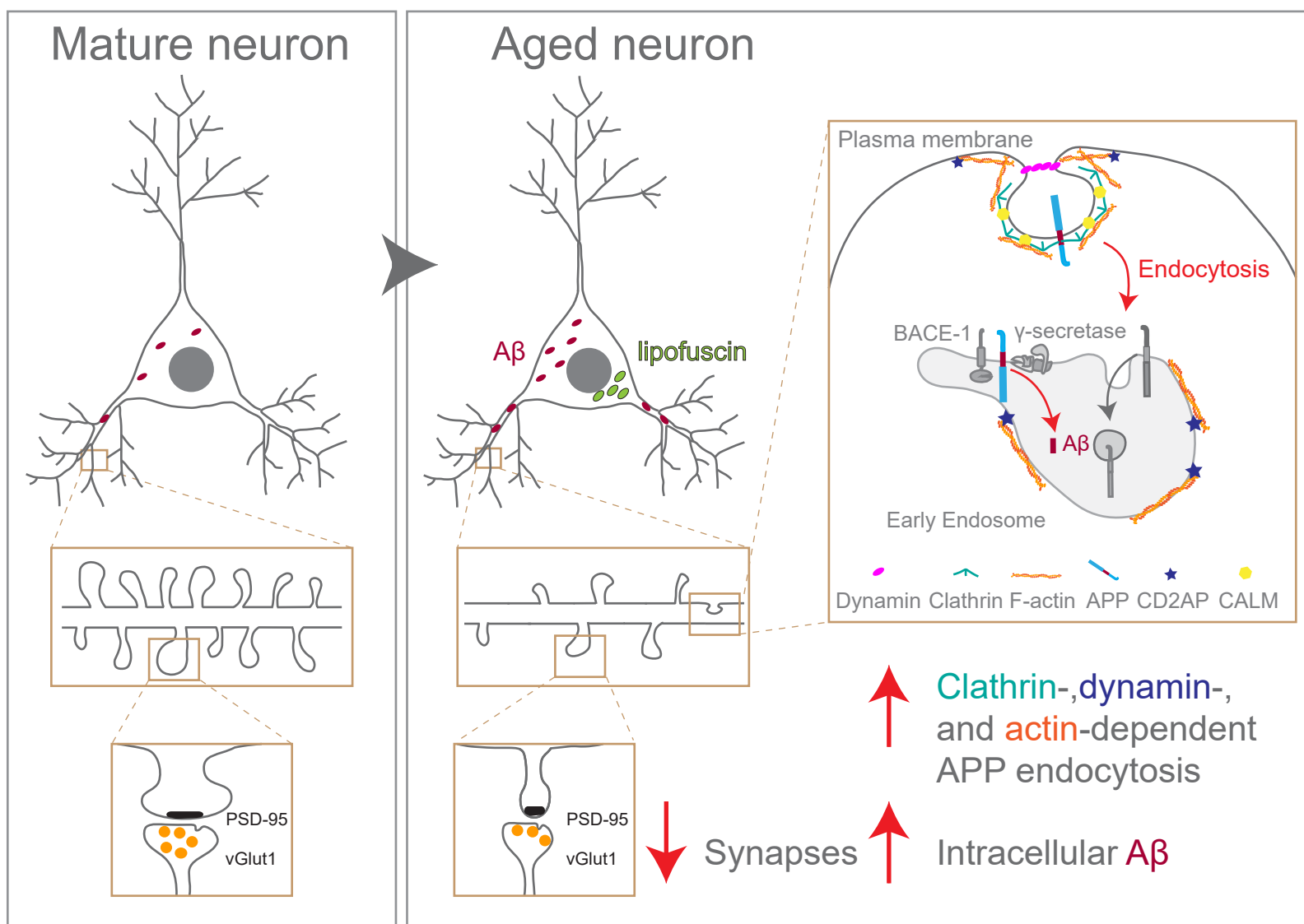


Figure S7. Schematics of APP endocytosis up-regulation and synapse loss with aging

Neuronal aging up-regulates APP endocytosis by increasing clathrin assembly and F-actin polymerization, recruiting more APP endocytic adaptors (CD2AP and CALM) to endocytic sites in aged neurons. The increase in APP endocytosis, will enhance the encounter with its secretases, and potentiate A β production during neuronal aging eventually triggering synapse decline and favoring the development of late-onset Alzheimer's disease.

Table S1

(1) P values in Figure 1B

	21DIV	28DIV
14DIV	0.0432	0.0095

(2) P values in Figure 1E

	28DIV
21DIV	< 0.0001

(3) P values in Figure 1G

	28DIV
21DIV cell body	< 0.0001
21DIV neurites	0.9027

(4) P values in Figure 1I

	14DIV	21DIV	28DIV
cell body			
14DIV	-	0.2790	0.0158
21DIV	0.2790	-	0.3231
Neurites			
14DIV	-	> 0.9999	< 0.0001
21DIV	> 0.9999	-	< 0.0001

(5) P values in Figure 1K

	28DIV
21DIV cell body	0.6739
21DIV neurites	< 0.0001

(6) P values in Figure 2B

	21DIV	28DIV
14DIV	> 0.9999	0.0071
21DIV	-	0.0039

(7) P values in Figure 2C

	21DIV	28DIV
14DIV	> 0.9999	0.0811
21DIV	-	0.0094

(8) P values in Figure 2D

	21DIV	28DIV
14DIV	> 0.9999	0.0038
21DIV	-	0.0033

(9) P values in Figure 2E

	21DIV	28DIV
14DIV	0.0067	0.0050
21DIV	-	> 0.9999

(10)P values in Figure 2F

	21DIV	28DIV
14DIV	> 0.9999	0.0323
21DIV	-	0.0006

(11)P values in Figure 2G

	21DIV	28DIV
14DIV	> 0.9999	0.4146
21DIV	-	0.7539

(12)P values in Figure 2I

	18M
6M	0.0110

(13)P values in Figure 2J

	18M
6M	0.7562

(14)P values in Figure 2K

	18M
6M	0.1071

(15)P values in Figure 2L

	18M
6M	0.2269

(16)P values in Figure 2M

	18M
6M	0.0397

(17)P values in Figure 2N

	18M
6M	0.0024

(18)P values in Figure 3B

	28DIV
21DIV	0.3374

(19)P values in Figure 3C

	28DIV
21DIV	< 0.0001

(20)P values in Figure 3D

	28DIV
21DIV	< 0.0001

(21)P values in Figure 3F

	28DIV
21DIV	0.0857

(22)P values in Figure 3G

	28DIV
21DIV	< 0.0001

(23)P values in Figure 3H

	28DIV
21DIV	0.0138

(24)P values in Figure 3J

	28DIV
21DIV	0.0275

(25)P values in Figure 3L

	28DIV
21DIV	0.2275

(26)P values in Figure 3N

	18M
12M	0.0016

(27)P values in Figure 3O

	18M
12M	0.0002

(28)P values in Figure 3P

	18M
12M	0.0038

(29)P values in Figure 3R

	18M
12M	0.5225

(30)P values in Figure 3S

	18M
12M	0.0215

(31)P values in Figure 3T

	18M
12M	0.0008

(32)P values in Figure 4C

	28DIV
21DIV 10'	0.0476
21DIV 30'	0.0079

(33)P values in Figure 4D

	28DIV
21DIV	0.0210

(34)P values in Figure 4E

	28DIV
21DIV	0.4316

(35)P values in Figure 4H

	28DIV
21DIV	< 0.0001

(36)P values in Figure 4I

	28DIV
21DIV	< 0.0001

(37)P values in Figure 4J

	28DIV
21DIV	0.2159

(38)P values in Figure 4M

	28DIV
21DIV 10'	> 0.9999
21DIV 60'	> 0.9999
21DIV 120'	0.6000

(39)P values in Figure 4O

	28DIV
21DIV	0.0004

(40)P values in Figure 5B

	28DIV
21DIV	0.5795

(41)P values in Figure 5C

	28DIV
21DIV	0.0034

(42)P values in Figure 5D

	28DIV
21DIV	0.0353

(43)P values in Figure 5F

	28DIV
21DIV	< 0.0001

(44)P values in Figure 5H

	28DIV
21DIV	< 0.0001

(45)P values in Figure 5J

	18M
6M	0.1111

(46)P values in Figure 5L

	28DIV
21DIV	< 0.0001

(47)P values in Figure 5M

	28DIV
21DIV	< 0.0001

(48)P values in Figure 5N

	28DIV
21DIV	0.0003

(49)P values in Figure 6B

	28DIV DMSO
28DIV Pitstop2	< 0.0001
28DIV Dynasore	< 0.0001
28DIV CPZ	< 0.0001
28DIV CK-666	< 0.0001
28DIV SMIFH2	< 0.0001

(50)P values in Figure 6D

	28DIV
21DIV	0.0317

(51)P values in Figure 6F

	18M
6M	0.0317

(52)P values in Figure 6H

	28DIV
21DIV	< 0.0001

(53)P values in Figure 6I

	28DIV
21DIV	0.5745

(54)P values in Figure 6J

	28DIV
21DIV	> 0.9999

(55)P values in Figure 6L

	28DIV
21DIV	< 0.0001

(56)P values in Figure 6N

	28DIV
21DIV	< 0.0001

(57)P values in Figure 6P

	28DIV
21DIV	< 0.0001

(58)P values in Figure 6Q

	28DIV
21DIV	0.0344

(59)P values in Figure 7B

	28DIV
21DIV	< 0.0001
28DIV DAPT	0.0006

(60)P values in Figure 7D

	28DIV
21DIV	< 0.0001
28DIV BACE inhibitor IV	< 0.0001

(61)P values in Figure 7F

	28DIV	28DIV DAPT
21DIV	< 0.0001	< 0.0001
28DIV DAPT	< 0.0001	-

(62)P values in Figure 7G

	28DIV	28DIV DAPT
21DIV	< 0.0001	0.0002
28DIV DAPT	0.0483	-

(63)P values in Figure 7I

	21DIV Rab5-mCherry
21DIV mCherry	0.0171

(64)P values in Figure 7K

	21DIV Rab5-mCherry
21DIV mCherry	0.0428

(65)P values in Figure 7L

	21DIV Rab5-mCherry
21DIV mCherry	0.0002

(66)P values in Figure 7M

	21DIV Rab5-mCherry
21DIV mCherry	0.0385